

Hydrogenation and Redox Isomerization of Allylic Alcohols Catalyzed by a New Water-Soluble Pd–tetrahydrosalen Complex

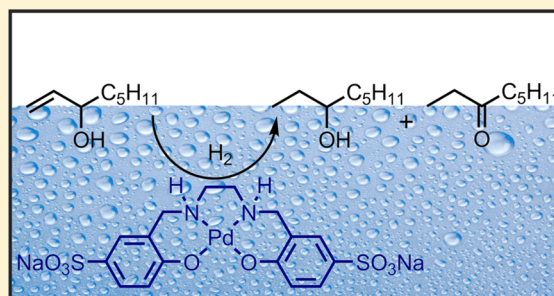
Krisztina Voronova,^{*,†} Mihály Purgel,[‡] Antal Udvardy,[†] Attila C. Bényei,[†] Ágnes Kathó,[†] and Ferenc Joó^{*,†,‡}

[†]Department of Physical Chemistry, University of Debrecen, Egyetem tér 1., H-4032 Debrecen, Hungary

[‡]MTA-DE Research Group on Homogeneous Catalysis and Reaction Mechanisms, P.O. Box 7, H-4010 Debrecen, Hungary

S Supporting Information

ABSTRACT: For applications in aqueous media, sulfonated tetrahydrosalen (sulfosalan, HSS) was synthesized by sulfonation of tetrahydrosalen in fuming sulfuric acid. The Pd(II) complex of this ligand, [Pd(HSS)], showed outstanding activity in hydrogenation and redox isomerization of allylic alcohols in homogeneous aqueous solutions or in aqueous–organic biphasic systems (for oct-1-en-3-ol TOF(hydrogenation) = 1580 h⁻¹, TOF(redox isomerization) = 400 h⁻¹). DFT calculations revealed that H₂ is activated heterolytically, resulting in a Pd(II)–hydride complex, [Pd(H)(HSS-Hphen)], in which one of the phenolate oxygens is protonated. Both hydrogenation and redox isomerization take place via concerted transfer of a proton and a hydride from the hydrogenated catalyst to the allylic alcohol.



1. INTRODUCTION

Transition-metal complexes of salen (double Schiff base of ethylenediamine and salicylaldehyde) play important roles as homogeneous and heterogeneous catalysts. The first such complexes were synthesized in 1933,¹ and since then several thousand salen-containing complexes have been prepared and characterized.² These compounds show catalytic activity in reactions such as the epoxidation of alkenes,³ ring opening of epoxides,⁴ the synthesis of cyclopropane⁵ and aziridine⁶ derivatives, etc. Many of these complexes are oxygen carriers; therefore, they can be regarded as models of metalloproteins.⁷ In addition, their fluorescent properties can be utilized for analytical and imaging purposes.⁸ In particular, Schiff base complexes of palladium proved to be active catalysts for hydrogenation⁹ and oxidation¹⁰ and in various C–C coupling reactions.¹¹

Interestingly, although [Pd(salen)] has been suggested as a synthetic model of hydrogenase,^{9a} due to its insolubility in water its properties could be studied only in ethanolic solutions.

Today's clean and green chemistry prefers the use of aqueous media. Since water is nontoxic and nonflammable, its application results in safer and cheaper processes. In many cases the products can be isolated from the reaction mixture by simple extraction, while the water-soluble catalyst can be reused in the aqueous phase. Aqueous organometallic catalysis¹² has become a standard procedure on both laboratory and industrial scales in reactions such as hydroformylation,¹³ hydrogenation,¹⁴ redox isomerization,¹⁵ C–C coupling,¹⁶ and many others.

Water-soluble salen complexes hitherto have been applied mostly for catalysis of oxidations;¹⁷ however, there are examples in the literature for N-arylations,¹⁸ coupling reactions,¹⁹ and

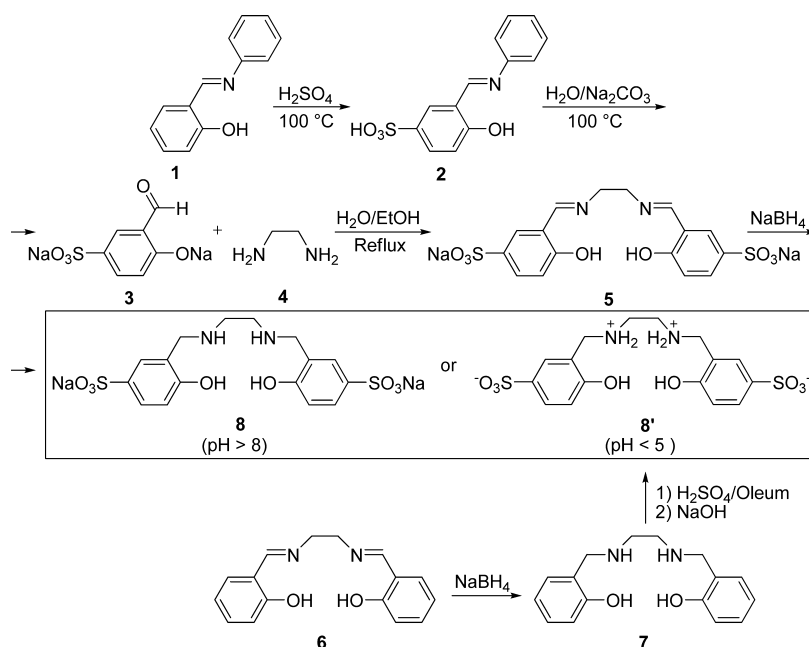
reductions²⁰ as well. Use of Schiff base ligands and their complexes in aqueous catalysis is hindered by their propensity to hydrolysis.²¹ Hydrogenation of the salen C=N bonds results in amines (salans) with much higher stability in aqueous solutions.^{21a} Transition-metal complexes with salen ligands were found to be active catalysts for oxidation²² and polymerization.²³ Nevertheless, the possibilities offered by the use of such complexes in aqueous organometallic catalysis are still largely unexplored.

Catalytic redox isomerization of allylic alcohols is a 100% atom economical reaction, allowing the synthesis of aldehydes and ketones without the need for separate oxidation and reduction steps.^{15,24} These reactions may take place at shorter reaction times and may result in less waste and energy consumption. Typical catalysts^{15,24,25} are complexes of Ru, Rh, Ir, and Fe, while complexes of Pd have scarcely been suggested for such purposes. Redox isomerization can be part of the hydrogenation of allylic alcohols, when the alcohol is first isomerized to a ketone or aldehyde and the saturated alcohol is obtained by hydrogenation of the C=O function of the latter. Several catalysts were found to be selective for isomerization with no or negligible activity for hydrogenation.²⁶

Organometallic catalysis has been dominated by phosphine and (recently) carbene ligands, which can stabilize lower oxidation states of transition metals often involved in catalytic cycles. Nevertheless, as the above examples show, multidentate N- and O-donor ligands can also be useful in catalysis. Therefore, with the aim of extending the use of salen complexes

Received: June 14, 2013

Scheme 1. Synthesis of Sulfonated Salan (Top) as Its Na Salt (HSS) (8) According to the Literature^{21a,27} and (Bottom) as the Zwitterionic Free Acid (8') by a Simplified Procedure Used in This Study



in aqueous organometallic catalysis, we have synthesized and characterized the water-soluble sulfonated salan ligand and its Pd(II) complex. The latter compound showed high catalytic activity in the redox isomerization of allylic alcohols in aqueous solutions and in aqueous–organic biphasic systems. DFT calculations revealed intimate details of the reaction mechanism.

2. RESULTS AND DISCUSSION

2.1. Synthesis and Characterization of sulfosalan and Its Pd(II) Complex, [Pd(HSS)], and Hydrogenation and Redox Isomerization of Allylic Alcohols Catalyzed by [Pd(HSS)].

2.1.1. Synthesis and Characterization of sulfosalan, HSS, and Its Pd(II) Complex, [Pd(HSS)]. Sulfosalan (8) has already been reported in the literature.^{21a} Its synthesis (Scheme 1, top) involved the sulfonation of salicylanilide (1) and removal of the aniline protecting group by hydrolysis, followed by reaction of sulfonated salicylaldehyde (3) with ethylenediamine (4), yielding sulfonated salen (5) as a crystalline solid.²⁷ In the last step of the synthesis of HSS (8), sulfosalen (5) was hydrogenated in aqueous solution using NaBH₄. (In the following the abbreviation HSS is used for the disodium salt of disulfonated tetrahydrosalan.) We have followed a different route, according to which salen (6) (also available commercially) was first obtained in the condensation reaction of salicylaldehyde and ethylenediamine, and this was reduced by NaBH₄ (Scheme 1, bottom). The resulting amine (7) was then sulfonated in fuming sulfuric acid. Adjusting the acidity of the sulfonation mixture to pH 5 leads to precipitation of disulfonated salan as the free acid in its zwitterionic form (8').

Altogether the modified procedure is simpler and the overall yield of 8' (29% based on 6) is higher than that of the literature method for 8 (7%), despite the low yield of the sulfonation step. Elemental analysis and ¹H NMR and ESI-MS spectroscopy showed the correct results for disulfonated salan. The white solid is sparingly soluble in water; in contrast, its Na⁺ salt

dissolves well in aqueous media and also in dimethyl sulfoxide (DMSO).

Crystals suitable for a single-crystal X-ray structure determination were obtained by slow crystallization of the free sulfonic acid from a water/DMSO mixture. The asymmetric unit contains half of the molecule (Figure S1, Supporting Information). Both the phenolic oxygens and the nitrogen atoms are protonated, and the resulting positive charge is neutralized by the sulfonate groups (Figure 1). The

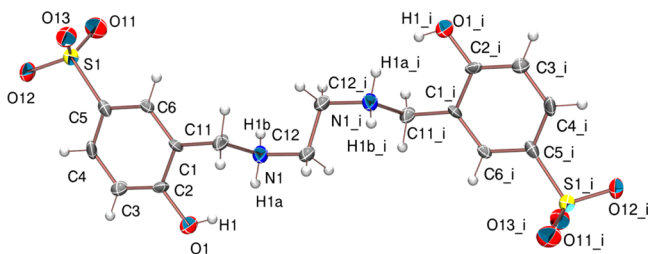


Figure 1. ORTEP view of sulfosalan (8') at the 50% probability level with the numbering scheme. The disordered dimethyl sulfoxide solvent is omitted for clarity. Selected bond distances (Å) and angles (deg): C12–C12(i) = 1.495(19), C11–N1 = 1.485(10), C12–N1 = 1.494(12), C5–S1 = 1.772(11), O11–S1 = 1.435(7), O12–S1 = 1.445(7), O13–S1 = 1.449(7); N1–C12–C12(i) = 109.9(11), O11–S1–O12 = 113.7(5), C2–O1–H1 (fixed angle) = 109.50. Symmetry code: (i) $-x, -y + 1, -z + 1$.

molecules in the crystal show a layered arrangement (Figure 2), with one DMSO between two sulfonated salan units, and this structure is stabilized by hydrogen bonds and π – π interactions. Bond distances and angles of sulfosalan show good agreement with the analogous parameters of similar molecules described in the literature.²⁸ The C11–N1 bond distance, 1.485(10) Å, refers to a single carbon–nitrogen bond. In the $-\text{CH}_2-\text{N}^+\text{H}_2-\text{CH}_2-$ part of the molecule all atoms are sp³-hybridized, similar to the structure of salen.²⁹

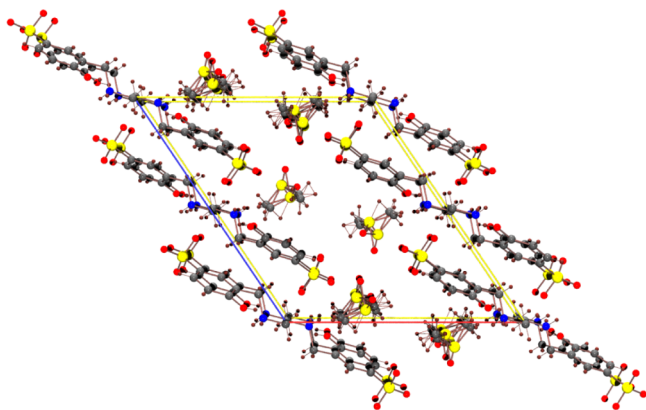
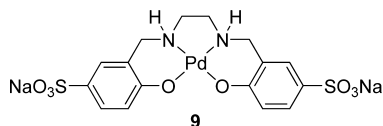


Figure 2. Packing diagram of sulfosalan molecules showing the layered structure and the cavity filled with disordered DMSO molecules. The structure is stabilized by hydrogen bonds and π - π interactions.

The Pd(II) complex of sulfosalan, [Pd(HSS)] (**9**) (Scheme 2), was prepared by stirring equimolar amounts of $(\text{NH}_4)_2[\text{PdCl}_4]$ and HSS in aqueous solution at pH 7.5 for 10 h at 60 °C followed by precipitation with ethanol.

Scheme 2. Pd(II)-sulfosalan (9**; [Pd-HSS])**



[Pd(HSS)] (**9**) is quite soluble in water and in DMSO but is insoluble in apolar organic solvents. Aqueous solutions of [Pd(HSS)] are stable in the air and can be stored for months. Due to the slow complex formation even at 60 °C, direct pH-potentiometric studies could not be carried out to determine the stability of the complex at various pHs. Above pH 6 no

reaction was observed with H_2 under pressures up to 9 bar (no metal formation was seen, and no Pd-hydride species could be detected by ^1H NMR spectroscopy). However, in more acidic solutions reaction with hydrogen resulted in the formation of a black precipitate and consequently all our investigations were done at $\text{pH} \geq 6.05$.

2.1.2. Catalytic Activity of [Pd(sulfosalan)] in Hydrogenation and Redox Isomerization of Allylic Alcohols. Exploratory experiments were carried out also with the Pd(II) complex of sulfonated salen. As expected, the complex was not stable and even at room temperature and at low hydrogen pressures readily visible metal precipitation occurred.

In contrast, [Pd(HSS)] was found to be stable above pH 6. This catalyst was used both as prepared in situ and as an isolated solid (see the Experimental Section). In both forms it catalyzed the hydrogenation and redox isomerization of allylic alcohols (Table 1). Importantly, no reaction occurred in the absence of hydrogen, and the conversion of allylic alcohols increased with increased hydrogen pressure (Figures S10 and S11, Supporting Information). A mercury test showed that the reactions were homogeneously catalyzed. According to the results, the reactions became faster with increasing chain length of the alk-1-en-3-ol substrates. Therefore, most of the further measurements were made with oct-1-en-3-ol. Note that due to the low solubility of oct-1-en-3-ol in water these reaction systems are liquid biphases; however, under our conditions the stirring speed did not influence the reaction rate. It is noteworthy that the catalyst is active also at high substrate loadings (S/C 2000, Table 1, entry 13).

The isolated solid [Pd(HSS)] showed substantially higher catalytic activity than the in situ catalyst (Table 1, entry 7 vs 10). Since the only difference between the two kinds of reaction mixtures was the presence of a stoichiometric amount of NH_4Cl in solutions of the in situ catalyst, we checked the effect of chloride on the rate of the reaction of oct-1-en-3-ol. As can be seen from Table 1 (entries 8 and 9), addition of NaCl

Table 1. Hydrogenation and Redox Isomerization of Allylic Alcohols^a

entry	catalyst	R ₁	R ₂	yield (%) ^b		TOF (h ⁻¹) ^h	
				11	12	hydrogenation	redox isomerization
1	in situ	H	H	19 ^c	2 ^c	38	4
2	in situ	CH ₃	H	7 ^c	3 ^c	14	6
3	in situ	H	CH ₃	26 ^c	6 ^c	52	12
4	in situ	H	C ₂ H ₅	54 ^c	17 ^c	108	34
5	in situ	H	C ₃ H ₇	70	16	140	32
6	in situ	H	C ₄ H ₉	70	17	140	34
7	in situ	H	C ₃ H ₁₁	71	19	142	38
8	isolated + NaCl (1:1)	H	C ₃ H ₁₁	83	13	166	26
9	isolated + NaCl (1:10)	H	C ₃ H ₁₁	78	14	156	28
10	isolated ^d	H	C ₃ H ₁₁	74	26	296	104
11	in situ ^e	H	C ₃ H ₁₁	36	10	144	40
12	isolated ^f	H	C ₃ H ₁₁	65	20	1300	400
13	isolated ^g	H	C ₃ H ₁₁	79	20	1580	400

^aConditions (except where noted): substrate (**10**), 0.25×10^{-3} mol; catalyst, 1.25×10^{-6} mol; 3 mL 0.2 M phosphate buffer, pH 6.05; 5 bar of H_2 ; 1 h; 80 °C. ^bYield determined by GC. ^cYield determined by ^1H NMR spectroscopy. ^d30 min. ^eCatalyst, 0.625×10^{-6} mol. ^fCatalyst, 1.25×10^{-7} mol. ^gCatalyst, 1.25×10^{-7} mol; 9 bar of H_2 . ^hTOF = (mol of product) / ((mol of catalyst) h⁻¹); in cases where the conversions of oct-1-en-3-ol are close to 100%, the given TOF's represent minimum values of catalytic activity.

decreased the catalytic activity of the isolated complex to about the level of the in situ prepared catalyst. This effect was not investigated in detail; however, it shows that coordinating ligands, such as chloride, may easily occupy free coordination site(s) on Pd and inhibit the catalytic process.

In addition to the redox isomerization process, under a hydrogen atmosphere [Pd(HSS)] can catalyze as well the hydrogenation of the C=C double bond in the allylic alcohol and that of the C=O double bond in the ketone product of isomerization. In general, under our conditions, formation of the saturated alcohol (**11**) took preference over that of ketone (**12**). At pH 6.05 the ratio of **12** in the product mixture was about 20% (Table 1); therefore, [Pd(HSS)] proved to be a better catalyst for hydrogenation than for redox isomerization.

Reactions of oct-1-en-3-ol under H₂ were studied in detail both with the in situ prepared and with the isolated [Pd(HSS)] catalysts, and the results are shown on Figures S6–S16 as Supporting Information. In aqueous systems, the pH of the catalyst solution may have a dramatic influence on the activity and selectivity of the catalyst.^{14e,30} With [Pd(HSS)] as catalyst, the overall conversion of oct-1-en-3-ol was only slightly effected by changes in the pH; however, there was a significant increase in the selectivity toward hydrogenation (**11**:**12** from 33:25 to 41:16, Figure S12). An increase of the hydrogen pressure resulted in an increased rate of overall conversion of **10**; however, this was mostly manifested in the production of **11** (Figure S10). The catalyst proved to be active also at high substrate loadings (no substrate or product inhibition was observed). Under the conditions of Figures S14 and S15 at 1 bar of H₂ pressure the activity varied according to a saturation curve and a limiting TOF around 650 h⁻¹ could be calculated (Figure S16).

Initial TOF values of the formation of octan-3-ol and octan-3-one were used for the calculation of overall activation energies of these two processes (Figure 3). It should be stressed

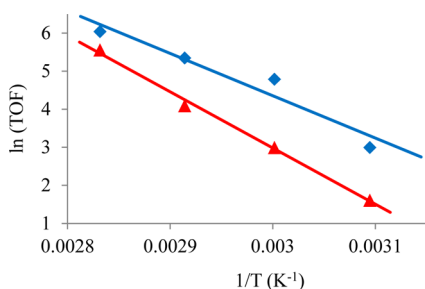


Figure 3. Hydrogenation and redox isomerization of oct-1-en-3-ol: Arrhenius plots for formation of octan-3-one (red \blacktriangle , $E_a = 87.2$ kJ/mol) and octan-3-ol (blue \blacklozenge , $E_a = 115.6$ kJ/mol). Conditions: substrate, 0.25×10^{-3} mol; isolated [Pd(HSS)], 2.5×10^{-7} mol; 3 mL 0.2 M phosphate buffer, pH 6.05; 1 bar of H₂; 60 min. The conversion was determined by GC.

that the obtained E_a values cannot be ascribed solely to chemical reactions. In this multiphase system the solubility of oct-1-en-3-ol and H₂ in the catalyst-containing aqueous phase may significantly modify the overall temperature dependence.

The time course of the product distribution (Figures S6 and S7) and its dependence on the hydrogen pressure (Figures S10 and S11) both indicated some, albeit low, reactivity of octan-3-one (**12**) toward hydrogenation under the reaction conditions employed. However, when the hydrogenation of **12** was attempted separately, no formation of octan-3-ol (**11**) was

detected. Nevertheless, in a mixture of **11** and **12**, hydrogenation of **12** also occurred to a considerable extent (Table 2).

Table 2. Hydrogenation of Octan-3-one and Octan-3-one/Oct-1-en-3-ol Mixtures^a

entry	substrate(s)	time (h)	11 (%) ^b
1	12	4	0
2	80% 12 + 20% 10	0.5 ^c	14
3	80% 12 + 20% 10	4 ^c	27

^aConditions (except where noted): substrate (**10**), 0.25×10^{-3} mol; catalyst, 6.5×10^{-7} mol; 3 mL of 0.2 M phosphate buffer, pH 6.05; 5 bar of H₂; 80 °C. ^bConversion determined by GC; ^cNo unreacted oct-1-en-3-ol left.

Although in the first 0.5 h of the reaction the amount of **11** was still less than that of the initially added **10**, after 4 h as much as 27% of **11** could be detected, 7% of which should have come from a slow hydrogenation of **12**.

As discussed above, [Pd(HSS)] showed high activity in the hydrogenation of allylic alcohols to saturated alcohols. Therefore, hydrogenation of the olefin oct-1-ene was also attempted. Surprisingly, under the conditions of Table 2 (but with 1 bar of H₂) only a 1% yield of octane was obtained in 4 h. Similar to the hydrogenation of **12**, addition of oct-1-en-3-ol (**10**) increased the rate of hydrogenation of oct-1-ene as well, and after 4 h 21% of octane could be detected, while oct-1-en-3-ol reacted to yield 45% of octan-3-ol and 55% of octan-3-one.

Liquid biphasic reaction systems allow isolation of the product and recycling of the catalyst by phase separation. In the [Pd(HSS)]-catalyzed redox isomerization of oct-1-en-3-ol, recycling experiments showed that the activity of the catalyst dropped significantly after the first reaction, followed by smaller changes in the consecutive runs (Table 3). After the fifth run

Table 3. Recycling of the Pd-sulfosalen Catalyst in Hydrogenation and Redox Isomerization of Oct-1-en-3-ol

no. of cycles	yield (%) ^b		TOF (h ⁻¹)	
	11	12	hydrogenation	redox isomerization
1	42	26	420	260
2	24	21	240	220
3	22	21	220	210
4	16	19	160	190
5	14	13	140	130

^aConditions: substrate, 0.25×10^{-3} mol; catalyst, 2.5×10^{-7} mol; 3 mL of 0.2 M phosphate buffer, pH 6.05; 1 bar of H₂; 1 h; 80 °C. ^bConversion determined by GC.

the catalyst still retained 40% of its original activity. Interestingly, while in the first run hydrogenation was preferred over isomerization, in the following runs the hydrogenated/isomerized product ratio was about 1. At present, the reason for this phenomenon is unclear.

2.1.3. Discussion of Experimental Results. In this paper we report a new synthesis of sulfonated tetrahydrosalen (sulfosalen, HSS) by direct sulfonation of tetrahydrosalen. Since salen is easily available either commercially or via a straightforward high-yield synthesis and moreover its hydrogenation with NaBH₄ can be easily accomplished, this new procedure represents a more efficient route to the water-soluble HSS in comparison to that published earlier.^{21a,27} In contrast to sulfonated salen, HSS is a water-stable compound. The Pd(II)

complex of this ligand was obtained by prolonged reaction of $(\text{NH}_4)_2[\text{PdCl}_4]$ in aqueous solution followed by precipitation with ethanol. Both HSS and $[\text{Pd}(\text{HSS})]$ can be stored in aqueous solution in the air for long periods (months).

Redox isomerization of allylic alcohols is an intensively studied, synthetically useful procedure.²⁴ Most of the known catalysts are based on iron, ruthenium, or rhodium.^{24,25,31} Only a few of these catalysts show activities in the range of several thousand turnovers per hour,³² while the most outstanding catalysts are characterized by turnover frequencies (TOF's) as high as 40000–50000 h^{-1} .³³ Nevertheless, in aqueous–organic biphasic systems the catalytic activity rarely exceeds $\text{TOF} = 1000 \text{ h}^{-1}$.

Although Pd/C polymer-supported Pd or Pd nanoparticles have been studied as catalysts for the redox isomerization of allylic alcohols³⁴ (with interesting solvent effects in case of Pd NP's),^{34d} soluble Pd complexes are not typical catalysts for this reaction, and only a few attempts have been made to use water-soluble Pd complexes in aqueous solutions or in aqueous–organic biphasic systems for such transformations. Blum and co-workers studied the catalytic properties of ion pairs obtained from PdSO_4 and Aliquat 336 in water and found a maximum $\text{TOF} = 4.8 \text{ h}^{-1}$ in the redox isomerization of oct-1-en-3-ol at 80 °C.³⁵ The catalytic activity of the complex obtained from PdSO_4 and sulfonated bis(diphenylphosphino)propane, DPPPS, was characterized by a $\text{TOF} = 228 \text{ h}^{-1}$ in biphasic isomerization of hex-1-en-3-ol in water/heptene at 50 °C.³⁶ It was gratifying, therefore, that $[\text{Pd}(\text{HSS})]$ catalyzed the hydrogenation/redox isomerization of various allylic alcohols under mild conditions with an overall activity in hydrogenation and redox isomerization of oct-1-en-3-ol up to $\text{TOF} = 1980 \text{ h}^{-1}$ at 9 bar of H_2 and 80 °C (Table 2, entry 13). This value exceeds most of the activities of hitherto reported Rh- and Ru-based catalysts and is exceptionally high for a palladium complex catalyst.

We did not attempt a detailed study of the reaction mechanism by experimental methods, such as e.g. detection of reaction intermediates. Nevertheless, the kinetic features of the reaction are in agreement with the general mechanisms proposed for such processes.^{15a,b} Accordingly, key species in the mechanism may be Pd hydrides, and this is corroborated by the finding that no reaction occurs in the absence of H_2 (at least up to 80 °C). The same finding is in opposition to the idea that the supposed Pd–hydride species can be formed by the interaction of $[\text{Pd}(\text{HSS})]$ and allylic alcohols, notably oct-1-en-3-ol. One may speculate, therefore, that the accelerating effect of **10** on the hydrogenation of both **12** and oct-1-ene may be more physical than chemical in nature: i.e., it originates from the slightly increased solubility of the substrates in water.

2.2. Study of the Catalytic Activity of Pd–Sulfosalan and the Mechanisms of Hydrogenation and Redox Isomerization Reactions by DFT Calculations. With the aim of obtaining a detailed insight into the mechanism of $[\text{Pd}(\text{HSS})]$ -catalyzed hydrogenation and redox isomerization of allylic alcohols, DFT calculations were performed. This method has already been used for the study of several salen-type complexes;³⁷ however, there have been only sporadic reports in the literature for complexes with salan ligands.³⁸ It was found that for palladium complexes correct results can be obtained by DFT calculations using the LanL2DZ effective core potential.^{39,40}

In general, hydrogenations can take place by three routes. The first possibility is in that the catalyst transfers a hydride ion

onto the substrate and this is followed by protonation of the latter.⁴⁰ In the second case, protonation is the first step followed by a hydride transfer.⁴¹ This may be unlikely in our systems, since the proton concentration is low ($\text{pH} \geq 6.05$). Finally, the proton and hydride may be transferred simultaneously.⁴² Bellarosa et al. studied the catalytic activity of Ru(II) complexes in the redox isomerization of allylic alcohols.⁴³ According to their calculations the reaction takes place by this third route: heterolytic hydrogenation of H_2 followed by concerted transfer of a proton and a hydride onto the substrate.

The experimental results described above showed that there was no significant rate increase of redox isomerization in the homologous series of alk-1-en-3-ols with more than six carbon atoms; therefore, hex-1-en-3-ol was chosen as the model substrate for theoretical calculations.

Figure 4 shows the structures of possible products of redox isomerization, hydrogenation, and dehydrogenation of hex-1-

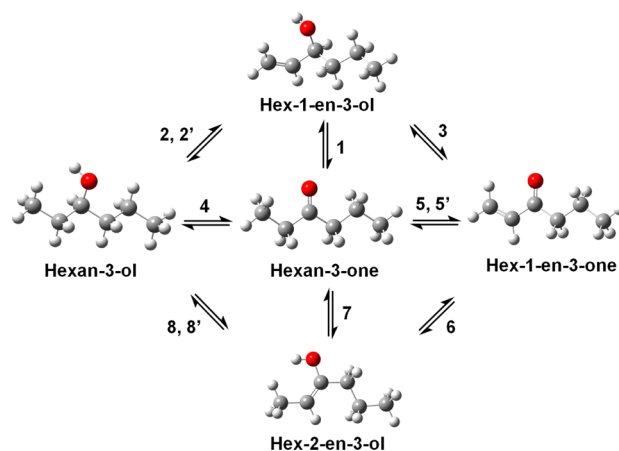
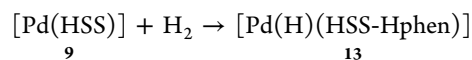


Figure 4. Equilibria of various species considered in calculations on catalytic hydrogenation and redox isomerization of hex-1-en-3-ol.

en-3-ol (only compounds in equilibrium are displayed). Depending on the proton transfer site (carbon 1 or 2), two products and two pathways (2 and 2') can be considered. In the following we examine the various pathways leading to the experimentally observed products.

2.2.1. Uncatalyzed Redox Isomerization of Hex-1-en-3-ol. In the absence of the Pd catalyst, redox isomerization of hex-1-en-3-ol to hexan-3-one (Figure 4, reaction 1) requires



participation of two solvent (water) molecules. The activation barrier of this route in vacuo is very high (+193.6 kJ/mol); however, the process is very favorable thermodynamically (−101.2 kJ/mol) (see Table 4). In the transition state the protons move in a concerted process. The exceptionally high activation barrier is due to the TS structure (Figure S17, Supporting Information), in which the proton moves far away from the alcoholic oxygen and takes a position very close to C1; meanwhile, the position of the hydrogen on C3 remains almost unchanged. Following the proton transfer a spontaneous internal hydride migration takes place, yielding hexan-3-one (Figure S18, Supporting Information).

2.2.2. Hydrogenation and Dehydrogenation of Hex-1-en-3-ol. Under hydrogen, with heterolytic activation of H_2 ,

Table 4. Energetics of the Various Steps (Figure 4) in Redox Isomerization of Hex-1-en-3-ol to Hexan-3-one^a

reaction	reaction no.	catalyst	hydride transfer to ^{b/} from ^c	H ⁺ transfer to ^{b/} from ^c	B3LYP/LanL2DZ/6-31g* [*]			
					in vacuo		PCM	
					ΔG^\ddagger	ΔG_r	ΔG^\ddagger	ΔG_r
hex-1-en-3-ol → hexan-3-one	1		carbon 2	carbon 1	+193.6	-101.2	+198.8	-97.1
hex-1-en-3-ol → hexan-3-ol	2	[Pd(H)(HSS-Hphen)]	carbon 1	carbon 2	+135.8	-120.9	+132.2	-148.6
hex-1-en-3-ol → hexan-3-ol	2'	[Pd(H)(HSS-Hphen)]	carbon 2	carbon 1	+144.3	-90.4	+142.6	-127.9
hex-1-en-3-ol → hex-1-en-3-one	3	[Pd(HSS)]	<i>carbon 3</i>	<i>oxygen</i>	+106.5	+7.5	+128.8	+61.2
hexan-3-ol → hexan-3-one	4	[Pd(HSS)]	<i>carbon 3</i>	<i>oxygen</i>	+105.6	-16.8	+121.6	+52.2
hex-1-en-3-one → hexan-3-one	5	[Pd(H)(HSS-Hphen)]	carbon 2	carbon 1	+144.5	-83.8		
hex-1-en-3-one → hexan-3-one	5'	[Pd(H)(HSS-Hphen)]	carbon 1	carbon 2				
hex-1-en-3-one → Hex-2-en-3-ol	6	[Pd(H)(HSS-Hphen)]	carbon 1	oxygen	+9.0	-72.2	+6.2	-111.3
hex-2-en-3-ol → hexan-3-one	7			carbon 2	+76.6	-65.6	+92.5	-61.4
hex-2-en-3-ol → hexan-3-ol	8	[Pd(H)(HSS-Hphen)]	carbon 2	carbon 3	+228.9	-25.5		
hex-2-en-3-ol → hexan-3-ol	8'	[Pd(H)(HSS-Hphen)]	carbon 3	carbon 2	+176.3	-64.1		

^aBoldface values belong to favorable reaction pathways. ^bRoman type indicates transfer to. ^cItalics indicate transfer from.

[Pd(HSS)] reacts to yield a Pd–hydride (eq 1; details of this process will be discussed separately), in which one of the phenolate oxygens picks up the resulting proton.

The structure of this hydride, [Pd(H)(HSS-Hphen)], is shown in Figure 5. In the presence of [Pd(H)(HSS-Hphen)]

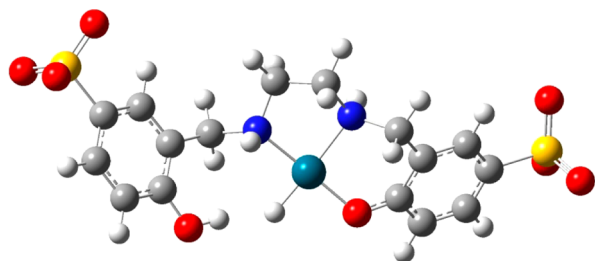


Figure 5. Structure of [Pd(H)(HSS-Hphen)] (13).

hex-1-en-3-ol can be hydrogenated to hexan-3-ol (Figure 4, routes 2 and 2', respectively), while its dehydrogenation with [Pd(HSS)] may supply hex-1-en-3-one (Figure S19, Supporting Information).

[Pd(HSS)] and [Pd(H)(HSS-Hphen)] are in equilibrium (although their precise population cannot be assessed by the calculations), and both can react with hex-1-en-3-ol. Similar to the results of Joubert and Delbecq,⁴² our calculations concluded that both hydrogenation and dehydrogenation take place via concerted processes.

Several attempts were made to separate the transfer of hydride and proton from the catalyst to the substrate. Considering the case when the substrate was protonated from the solvent, a spontaneous hydride transfer occurred to the adjacent carbon atom. In the case of protonation of the substrate by the phenolic H⁺ either a spontaneous hydride transfer or back-migration of H⁺ to the phenolate was observed, depending on the distance of the adjacent carbon atom in the substrate and the hydride. When hydride transfer was considered as the initial step of hydrogenation, the same

results were obtained. On the basis of these findings it can be concluded that addition of hydrogen to the substrate (without considering the effect of water molecules) happens via concerted addition of a hydride and a proton.

The interaction of [Pd(H)(HSS-Hphen)] with hex-1-en-3-ol may take place in two possible ways (Figure 4, reactions 2 and 2'): i.e., the proton and hydride may be transferred either to C1 or to C2 of the substrate. Figure 6 shows the transition states

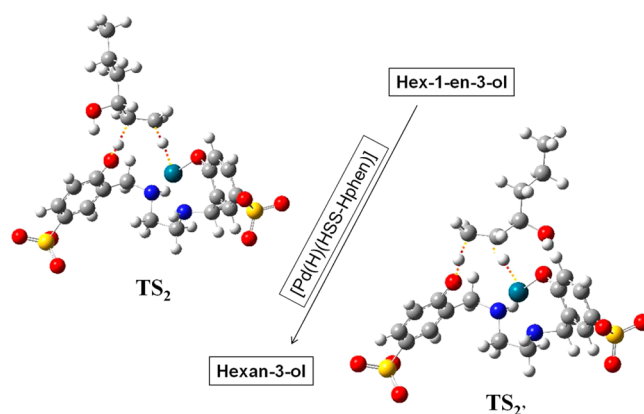


Figure 6. Two possible pathways of hydrogenation of hex-1-en-3-ol catalyzed by [Pd(H)(HSS-Hphen)].

(TS₂ and TS₂'). The activation barriers are high in both cases; however, both processes are very favorable thermodynamically (Table 4). Note that the hydrogen of the alcoholic –OH establishes a hydrogen bond with either the free phenol (TS₂) or coordinated phenolate (TS₂') oxygen. Of course, in a real dynamic system these are only two of the endless possibilities, where the hydrogen-bonding ability of the H₂O molecules in the aqueous solution should also be considered.

Hex-1-en-3-ol and hexan-3-ol may react with [Pd(HSS)] (Figure 4, reactions 3 and 4). In these cases there is only a single pathway for each of the reactions, i.e. the alcoholic –OH

protonates one of the coordinated phenol oxygens while a hydride is transferred from C3 to the palladium; altogether this leads to the formation of carbonyl compounds.

In summary, the reaction of hex-1-en-3-ol may supply three products. According to the calculations, direct redox isomerization (Figure 4, reaction 1) is very unfavorable. Formation of hexan-3-ol in a reaction with [Pd(H)(HSS-Hphen)] (Figure 4, reactions 2 and 2') has a slightly higher activation barrier than formation of hex-1-en-3-one from hex-1-en-3-ol and [Pd-(HSS)] (Figure 4, reaction 3); however, it is much more favored thermodynamically. Furthermore, it is strongly exothermic, in contrast to the formation of hex-1-en-3-one, which was found to be slightly endothermic. Consequently, the key step in the isomerization of hex-1-en-3-ol is the transformation of hexan-3-ol to hexan-3-one (Figure 4, reaction 4). This was found to be slightly exothermic with a not too high activation barrier, which suggests the hex-1-en-3-ol \rightarrow hexan-3-ol \rightarrow hexan-3-one channel as the major path of isomerization of the allylic alcohol to ketone.

2.2.3. Hydrogenation/Dehydrogenation of Hex-1-en-3-one. Although in the previous section it was concluded that hex-1-en-3-one does not play an important role in the formation of hexan-3-one, its hydrogenation still can contribute to the overall redox isomerization process. This hydrogenation may take place by hydride transfer from [Pd(H)(HSS-Hphen)] either onto the C1 or onto the C2 carbon of the enone. In the calculations we first determined the transition state of the concerted hydride/proton transfer step and then looked for the reactant and the product by geometry optimization of structures close to the transition state by small displacements of the proton and hydride. In this way we managed to calculate a free energy value only for the C2 hydride route (Figure 4, reaction 5), since the reactant of the C1 hydride route (Figure 4, reaction 5') is not consistent with the transition state.

The calculations led to the discovery of an unusual structure (Figure 7), which also suggested a new reaction pathway. It is

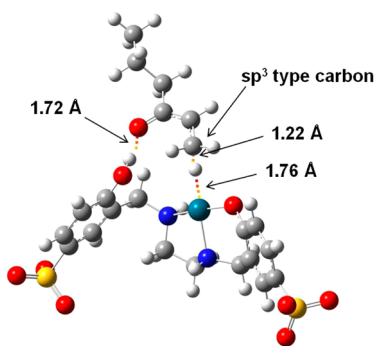


Figure 7. Structure of the reactant derived from β -hydride transfer.

not surprising that the ketone oxygen is involved in hydrogen bonding with the phenol hydrogen; however, the distance of the hydride ion from the Pd center was found to be about 20 pm longer (176.5 pm) than in all other structures involving [Pd(H)(HSS-Hphen)]. At the same time, the hydride established a very strong bond (122.2 pm) with the C1 carbon of the substrate, resulting in the loss of the sp^2 character of this carbon atom. As a consequence, the carbonyl bond became longer and the C–C bond distances were between those of characteristic C–C and C=C bond lengths.

Considering this unusual intermediate, there is a preferred reaction pathway (Figure 4, reaction 6) which is favored over the C2 hydride route both kinetically and thermodynamically. In this reaction step, in addition to the C1 hydride migration, a proton is transferred to the ketone oxygen and the product of the transformation is hex-2-en-3-ol. With the participation of H_2O molecules this vinylic alcohol rearranges to hexan-3-one (Figure 4, reaction 7). Isomerization processes of hex-2-en-3-ol to hexan-3-ol (Figure 4, reactions 8 and 8') have much higher activation barriers; therefore, they need not be considered in the overall isomerization process. The transformation of hexan-3-ol to hex-2-en-3-ol is even less favorable; thus, this reaction channel can be discarded.

2.2.4. Discussion of the Results of Theoretical Studies. The above theoretical calculations suggested that the major pathway of redox isomerization of the chosen substrate was the hex-1-en-3-ol \rightarrow hexan-3-ol \rightarrow hexan-3-one channel and this pathway could be supplemented to a minor extent by the hex-1-en-3-ol \rightarrow hex-1-en-3-one \rightarrow hex-2-en-3-ol \rightarrow hexan-3-one reaction sequence. These conclusions are in agreement with the experimental findings in that only hexan-3-ol and hexan-3-one were found in the reaction mixtures.

The theoretical model investigated above has three critical points. First is the chosen level of theory: the error introduced by the actual choice can only be guessed and, in addition, it is dependent on the system under investigation. The second uncertainty—as was mentioned before—is the population ratio of the [Pd(HSS)] and [Pd(H)(HSS-Hphen)] forms of the catalyst. Third, the energetics of reactants, transition states, and products were calculated for the gaseous state, with no involvement of solvent molecules; therefore, the final structures arrived at by geometry optimizations may be significantly different in the real reaction systems. It is obvious that errors of the calculation of activation barriers or reaction free energy values may influence the favorable/unfavorable nature of certain reaction steps, and reactions calculated as slightly exergonic or endergonic in reality may proceed in other directions.

In order to get a deeper insight into the energetics of redox isomerizations of hex-1-en-3-ol (and to check the reliability of the above results), we performed calculations with various theoretical methods. PCM calculations showed a significant destabilization of the ketone structures, leading to a less favorable hexan-3-ol \rightarrow hexan-3-one transformation (regarded above as the key step of the overall reaction). This is in agreement with the experimentally found higher ratio of hexan-3-ol in the product mixture. Notwithstanding, application of PCM results in significant energetic changes of the various routes (Table 4); moreover, the method does not consider the stabilizing effects of hydrogen bonds formed in aqueous solutions. In addition, the hexan-3-ol \rightarrow hexan-3-one reaction was studied in detail by calculations (geometry optimizations) for the gas phase, where the basis set, functionals, and ECP were varied. In all cases—similar to the results provided by the initial level of theory—the reaction was found to be slightly endergonic. Energetics of the equilibrium processes (Figure 4) are displayed in Tables 4 and 5.

On the basis of the above DFT calculations the following can be concluded (with reference to Figure 4). Direct redox isomerization of hex-1-en-3-ol to hexan-3-one is very unlikely, even with the assistance of water molecules (at least in vacuo). The major pathway of formation of hexan-3-ol is the reaction of hex-1-en-3-ol with [Pd(H)(HSS-Hphen)] (routes 2 and 2').

Table 5. Energetics of the Hexan-3-ol → Hexan-3-one Transformation in the Gas Phase Calculated by Various Theoretical Methods

level of theory	ΔG^\ddagger (kJ/mol)	ΔG_r (kJ/mol)
B3LYP/LanL2DZ/6-31g*	+105.6	-16.8
B3LYP/LanL2DZ/6-311+g**	+99.9	-16.3
B3LY/SDD/6-31g*	+113.4	-12.6
B3LYP/CRENBL/6-31g*	+110.7	-13.0
B2PLYP/LanL2DZ/6-31g*	+135.2	-19.5
M062X/LanL2DZ/6-31g*	+111.6	-29.2

There may be two channels of molecular transformations leading from hex-1-en-3-ol to hexan-3-one. The first is the dehydrogenation of hexan-3-ol (route 4) formed in the previous step. Nevertheless, there is another channel involving the dehydrogenation of hex-1-en-3-ol to hex-1-en-3-one (route 3), hydrogenation of the latter to hex-2-en-3-ol (route 6), and rearrangement of this vinylic alcohol to hexan-3-one (route 7). Although hex-1-en-3-one and hex-2-en-3-ol were not observed experimentally, the calculated free energies do not exclude the contribution of this channel to the overall reaction. This contribution may not be very extensive, though, since [Pd(HSS)] did not catalyze the redox isomerization of allylic alcohols in the absence of H_2 . Interestingly, on all theoretical levels, calculations show the preference of ketone formation over alcohol production; however, the solution model prefers unequivocally the formation of hexan-3-ol. This is what was found experimentally as well.

In conclusion, we have shown that disulfonated tetrahydro-salen formed a water-soluble Pd(II) complex with high stability in aqueous solution in the appropriate pH range. The complex was found to be active in hydrogenation and in the redox isomerization of allylic alcohols under mild conditions, with somewhat higher activity in hydrogenation than in redox isomerization. These findings open the way toward using transition-metal complexes with the versatile salan-type ligands as catalysts in aqueous solutions or aqueous-organic biphasic systems also for reactions other than the traditionally studied oxidations. Indeed, our recent experiments showed that [Pd(HSS)] was an active catalyst for various C–C coupling processes; these results will be reported in due course.

3. EXPERIMENTAL SECTION

3.1. General Conditions. All reagents were obtained commercially and used as received. Catalytic experiments were performed in high-pressure glass reactors. The 1H and ^{13}C NMR spectra of samples were recorded on a Bruker Avance 360 MHz spectrometer. Coupling constants are reported in Hz. ESI mass spectra were recorded on a Bruker micrOTOFQ ESI-TOF mass spectrometer. Reaction mixtures in hydrogenation and redox isomerization of allylic alcohols were analyzed by gas chromatography (Agilent 7890A gas chromatograph; HP-5 30 m \times 0.32 mm \times 0.25 μ m; FID; carrier gas nitrogen) or 1H NMR spectroscopy. Elemental analysis was carried out on an Elementar varioMicro cube instrument (CHNS).

3.2. Single-Crystal X-ray Structure Determinations. X-ray diffraction data of the sulfosalan ligand were collected at 293(2) K on a Bruker-Nonius MACH3 diffractometer equipped with a point detector using graphite-monochromated Mo $K\alpha$ radiation ($\lambda = 0.71073$ Å). The structure was solved by the SIR-92 program⁴⁴ and refined by full-matrix least-squares methods on F^2 , with all non-hydrogen atoms refined with anisotropic thermal parameters using the SHELXL-97 package.⁴⁵ Publication material was prepared with the WINGX suite.⁴⁶ All hydrogen atoms were located geometrically and refined in the riding mode, except for amine and alcoholic protons, which could be

found in the difference electron density map but their distance to the nitrogen/oxygen atom was constrained. Disorder of the solvent DMSO molecules was modeled using restrictions. These molecules occupy two places in the ratio 65:35. Further details of the structure determination can be found in the Supporting Information.

3.3. Synthesis of salen (6). The Schiff base salen ligand was prepared according to a literature procedure⁴⁷ by reaction of salicylaldehyde with ethylenediamine (2:1) in methanol. Yield: 10.12 g, 74% (37.72 mmol), yellow solid. 1H NMR (d_6 -DMSO, 360 MHz, δ): 3.96 (s, 4H, $-CH_2CH_2-$), 6.90 (q, $J = 7.9$ Hz, 4H, CH_{arom}), 7.35 (t, $J = 7.5$ Hz, 2H, CH_{arom}), 7.46 (d, $J = 7.5$ Hz, 2H, CH_{arom}), 8.62 (s, 2H, $CH=N$).

3.4. Synthesis of salan (7). The reduced Schiff base was prepared according to a literature procedure^{21a} by reducing the salen with $NaBH_4$ in dichloromethane. Yield: 10.14 g, 98% (37.23 mmol), white solid. 1H NMR (d_6 -DMSO, 360 MHz, δ): 3.38 (s, 4H, $-CH_2CH_2-$), 4.14 (s, 4H, CH_2-NH), 6.87 (t, $J = 7.0$ Hz, 2H, CH_{arom}), 7.02 (d, $J = 7.8$ Hz, 2H, CH_{arom}), 7.21 (t, $J = 7.6$ Hz, 2H, CH_{arom}), 7.46 (d, $J = 6.7$ Hz, 2H, CH_{arom}).

3.5. Synthesis of sulfosalan (8). To a mixture of 4 mL of 30% fuming sulfuric acid (oleum) and 1 mL of concentrated sulfuric acid was added salan (1.00 g, 3.67 mmol) in small portions. The mixture was stirred for 30 min. Then the content of the flask was carefully added to 25 mL of cooled water. The pH of the reaction mixture was set to 5 with 5 M NaOH solution. Then the mixture was cooled for 4–5 h, during which a white precipitate formed. The solid was collected by filtration, washed with cold water, and dried with diethyl ether. Crystals suitable for a single-crystal X-ray structure determination were obtained by slow crystallization of the ligand from a water/DMSO mixture. Yield: 524 mg, 30% (1.10 mmol). 1H NMR (D_2O , 360 MHz, δ): 2.67 (s, 4H, $-CH_2CH_2-$), 3.58 (s, 4H, CH_2-NH), 6.52 (d, $J = 8.6$ Hz, 2H, CH_{arom}), 7.36 (dd, $J_1 = 8.6$ Hz, $J_2 = 2.1$ Hz, 2H, CH_{arom}), 7.41 (d, $J = 2.1$ Hz, 2H, CH_{arom}). ^{13}C NMR (D_2O , 75 MHz, δ): 168.72, 127.69, 126.80, 126.31, 126.18, 118.43, 48.69, 47.25. ESI-MS for $C_{16}H_{18}Na_2N_2O_8S_2$ (m/z): calcd for $[M - 2Na + H]^+$ 431.059, found 431.064 (for the correct isotope distribution, see Figure S3 in the Supporting Information). Anal. Found (calcd) for $C_{16}H_{18}Na_2N_2O_8S_2 \cdot 2H_2O$ (512.38): C, 37.55 (37.51); H, 4.68 (4.33); N, 5.48 (5.47); S, 13.23 (12.52).

3.6. Synthesis of [Pd(HSS)] (9). A 114.3 mg portion (0.24 mmol) of sulfosalan and 73.9 mg (0.26 mmol) of $(NH_4)_2[PdCl_4]$ were dissolved in water (4 mL). The pH was set to 7.5 with 5 M NaOH, and the reaction mixture was stirred at 60 °C for 10 h. Then the solution was cooled and ethanol (20 mL) was added. The solid was filtered, washed with ethanol, and dried under vacuum. Yield: 135 mg, 97% (0.23 mmol). 1H NMR (D_2O , 360 MHz, δ): 2.78 (d, $J = 8.0$ Hz, 2H, $-CH_2CH_2-$), 2.94 (d, $J = 8.0$ Hz, 2H, $-CH_2CH_2-$), 3.46 (d, $J = 13.0$ Hz, 2H, CH_2-NH), 4.15 (d, $J = 13.2$ Hz, 2H, CH_2-NH), 6.81 (d, $J = 8.9$ Hz, 2H, CH_{arom}), 7.41 (s, 2H, CH_{arom}), 7.45 (d, $J = 9.2$ Hz, 2H, CH_{arom}). ^{13}C NMR (D_2O , 75 MHz, δ): 165.14, 129.22, 128.10, 127.58, 123.59, 118.86, 53.15, 53.01. ESI-MS $C_{16}H_{16}Na_2N_2O_8S_2Pd$ (m/z): calcd for $[M - 2Na]^{2+}$ 266.970, found 266.967 (for the correct isotope distribution, see Figure S5 in the Supporting Information). Anal. Found (calcd) for $C_{16}H_{16}Na_2N_2O_8S_2Pd \cdot 10H_2O$ (778.83): C, 24.68 (24.68); H, 4.55 (4.92); N, 3.65 (3.60); S, 8.60 (8.23).

3.7. In Situ Preparation of [Pd(HSS)] (9). A 47.6 mg portion (0.1 mmol) of sulfosalan and 28.4 mg (0.1 mmol) of $(NH_4)_2[PdCl_4]$ were dissolved in water (10 mL). The pH was set to 7.5 with 5 M NaOH, and the solution was stirred at 60 °C for 10 h. With time the brown mixture turned yellow. λ_{max}/nm ($\epsilon/M^{-1} cm^{-1}$): 256 (48500), 320 (21490).

3.8. General Procedure for Hydrogenation and Redox Isomerization of Allylic Alcohols. A solution of the catalyst (0.625×10^{-2} to 0.83×10^{-4} mmol) in water (100–125 μ L), allylic alcohol (0.25 mmol), and 3 mL of 0.2 M Na-phosphate buffer of appropriate pH were placed into a high-pressure tube. The tube was evacuated then filled with 1–9 bar of H_2 . The reaction vessel was immersed into a thermostated bath (40–80 °C), and the mixture was stirred for 15–210 min. At room temperature the products were extracted with 1 mL of chloroform, dried over $MgSO_4$, and subjected

to gas chromatography. The conversion of water-soluble allylic alcohols and the yields of products were determined by ^1H NMR spectroscopy. In the recycling experiments after the extraction the catalyst-containing aqueous phase was used in the next run.

3.9. Computational Methods. All calculations were performed employing DFT using the Gaussian 09 package.⁴⁸ Full geometry optimizations of the systems were performed in vacuo, and single-point calculations were done in solution using the polarizable continuum model (PCM).⁴⁹ We have used exchange correlation hybrid functionals B3LYP⁵⁰ and M062X⁵¹ and the double-hybrid method B2PLYP⁵² for the calculations. For hydrogen, carbon, nitrogen, oxygen, and chloride atoms the 6-31G(d) and the 6-311+G(d,p) basis sets⁵³ were used. Relativistic effects of the metal ions were considered through the use of the LanL2DZ,⁵⁴ SDD⁵⁵ and CRENL⁵⁶ relativistic effective core potentials (RECP) with the related valence basis sets. The transition states of the mechanisms were investigated in vacuo by means of the synchronous transit-guided quasi-Newton method.⁵⁷ The stationary points found on the potential energy surfaces as a result of the geometry optimizations have been tested to represent energy minima rather than saddle points via frequency analysis. The relative energy barriers include non-potential-energy contributions (that is, zero-point energies and thermal terms) obtained by frequency analysis.

■ ASSOCIATED CONTENT

■ Supporting Information

Figures and tables giving the asymmetric unit of the sulfosalan ligand, crystallographic data, NMR and ESI-MS spectra, detailed experimental results of the reactions of oct-1-en-3-ol under H_2 with both the in situ prepared and the isolated $[\text{Pd}(\text{HSS})]$ catalyst, and optimized geometries and a CIF file giving crystallographic data for the HSS ligand. This material is available free of charge via the Internet at <http://pubs.acs.org>.

■ AUTHOR INFORMATION

Corresponding Author

*E-mail: joo.ferenc@science.unideb.hu (F.J.); voronova.kristina@science.unideb.hu (K.V.).

Notes

The authors declare no competing financial interest.

■ ACKNOWLEDGMENTS

This paper is dedicated to Professor Irina Petrovna Beletskaya for her outstanding contributions to metal-catalyzed reactions. This work was supported by the National Research Fund of Hungary (OTKA 101372) and by the grants TÁMOP-4.2.2.A-11/1/KONV-2012-0043 (ENVIKUT) and TÁMOP-4.2.2.C-11/1/KONV-2012-0010 (Supercomputer, the national virtual laboratory) cofinanced by the European Union and the European Social Fund. We are grateful to Dr. Attila Kiss for the elemental analyses and to Dr. Lajos Nagy for the ESI-MS measurements.

■ REFERENCES

- (1) Pfeiffer, P.; Breith, E.; Lübke, E.; Tsumaki, T. *Liebigs Ann. chem.* **1933**, *503*, 84–130.
- (2) (a) Dalton, C. T.; Ryan, K. M.; Wall, V. M.; Bousquet, C.; Gilheany, D. G. *Top. Catal.* **1998**, *5*, 75–91. (b) Baleizão, C.; Garcia, H. *Chem. Rev.* **2006**, *106*, 3987–4043. (c) Gupta, K. C.; Sutar, A. K. *Coord. Chem. Rev.* **2008**, *252*, 1420–1450. (d) Kleij, A. W. *Eur. J. Inorg. Chem.* **2009**, *2*, 193–205. (e) Jones, C. W. *Top. Catal.* **2010**, *53*, 942–952. (f) Zhou, Q.-L.; Zhang, W.-Z.; Lu, X.-B. *Privileged Chiral Ligands and Catalysts*; Wiley-VCH: Weinheim, Germany, 2011. (g) Crane, A. K.; MacLachlan, M. J. *Eur. J. Inorg. Chem.* **2012**, *1*, 17–30. (h) Whiteoak, C. J.; Salassa, G.; Kleij, A. W. *Chem. Soc. Rev.* **2012**,

41, 622–631. (i) Mechler, M.; Latendorf, K.; Frey, W.; Peters, R. *Organometallics* **2013**, *32*, 112–130.

(3) (a) Jacobsen, E. N.; Zhang, W.; Muci, A. R.; Ecker, J. R.; Deng, L. *J. Am. Chem. Soc.* **1991**, *113*, 7063–7064. (b) Jacobsen, E. N.; Zhang, W.; Guler, M. L. *J. Am. Chem. Soc.* **1991**, *113*, 6703–6704. (c) Bhunia, A.; Gotthardt, M. A.; Yadav, M.; Gamer, M. T.; Eichhöfer, A.; Kleist, W.; Roesky, P. W. *Chem. Eur. J.* **2013**, *19*, 1986–1995. (d) Maity, N. Ch.; Rao, G. V. S.; Prathap, K. J.; Abdi, S. H. R.; Kureshy, R. I.; Khan, N. H.; Bajaj, H. C. *J. Mol. Catal. A: Chem.* **2013**, *366*, 380–389.

(4) (a) Martinez, L. E.; Leighton, J. L.; Carsten, D. H.; Jacobsen, E. N. *J. Am. Chem. Soc.* **1995**, *117*, 5897–5898. (b) DiCiccio, A. M.; Coates, G. W. *J. Am. Chem. Soc.* **2011**, *133*, 10724–10727. (c) Venkatasubbiah, K.; Feng, Y.; Arrowood, T.; Nickias, P.; Jones, C. W. *ChemCatChem* **2013**, *5*, 201–209.

(5) (a) Jason, A. M.; Wiechang, J.; SonBinh, T. N. *Angew. Chem., Int. Ed.* **2002**, *41*, 2953–2956. (b) Falkowski, J. M.; Wang, C.; Liu, S.; Lin, W. *Angew. Chem., Int. Ed.* **2011**, *50*, 8674–8678. (c) Uehara, M.; Suematsu, H.; Yasutomi, Y.; Katsuki, T. *J. Am. Chem. Soc.* **2011**, *133*, 170–171.

(6) (a) Li, Z.; Conser, K. R.; Jacobsen, E. N. *J. Am. Chem. Soc.* **1993**, *115*, 5326–5327. (b) Fukunaga, Y.; Uchida, T.; Ito, Y.; Matsumoto, K.; Katsuki, T. *Org. Lett.* **2012**, *14*, 4658–4661.

(7) Jarson, E. J.; Pecoraro, V. L. In *Manganese Redox Enzymes*; Pecoraro, V. L., Ed.; VCH: New York, 1992; pp 1–28.

(8) (a) Cozzi, P. G.; Dolci, L. S.; Garelli, A.; Montalti, M.; Prodi, L.; Zaccheroni, N. *New J. Chem.* **2003**, *27*, 692–697. (b) Zhou, L.; Cai, P.; Feng, Y.; Cheng, J.; Xiang, H.; Liu, J.; Wu, D.; Zhou, X. *Anal. Chim. Acta* **2012**, *735*, 96–106.

(9) (a) Henrici-Olivé, G.; Olivé, S. *Angew. Chem.* **1974**, *13*, 549–550. (b) Kowalak, S.; Weiss, R. C.; Balkus, K. J., Jr. *J. Chem. Soc., Chem. Commun.* **1991**, *1*, 57–58. (c) Ernst, S.; Fuchs, E.; Yang, X. *Microporous Mesoporous Mater.* **2000**, *137*, 35–36. (d) Tas, E.; Kilic, A.; Durgun, M.; Yilmaz, I.; Özdemir, I.; Gurbuz, N. *J. Organomet. Chem.* **2009**, *694*, 446–454. (e) Islam, S. M.; Roy, A. S.; Mondal, P.; Salam, N. *Appl. Organomet. Chem.* **2012**, *26*, 625–634.

(10) (a) Dileep, R.; Bhat, B. R. *Appl. Organomet. Chem.* **2010**, *24*, 663–666. (b) Ravi Krishna, E.; Muralidhar Reddy, P.; Sarangapani, M.; Hanmanthu, G.; Geeta, B.; Shoba Rani, K.; Ravinder, V. *Spectrochim. Acta, Part A* **2012**, *97*, 189–196. (c) Dayan, S.; Kalaycioglu, N. O. *Appl. Organomet. Chem.* **2012**, *27*, 52–58.

(11) (a) Borhade, S. R.; Waghmode, S. B. *Tetrahedron Lett.* **2008**, *49*, 3423–3429. (b) Bakherad, M.; Keivanloo, A.; Bahramian, B.; Hashemi, M. *Tetrahedron Lett.* **2009**, *14*, 1557–1559. (c) Borhade, S. R.; Waghmode, S. B. *Indian J. Chem.* **2010**, *49B*, 565–572. (d) Liu, P.; Feng, X.-J.; He, R. *Tetrahedron* **2010**, *66*, 631–636. (e) Matos, M. J.; Vazquez-Rodriguez, S.; Borges, F.; Santana, L.; Uriarte, E. *Tetrahedron Lett.* **2011**, *52*, 1225–1227. (f) Zhou, Z.; Zhou, Z.; Chen, A.; Zhou, X.; Qi, Q.; Xie, Y. *Transition Met. Chem.* **2013**, *38*, 401–405.

(12) (a) Joó, F. *Aqueous Organometallic Catalysis*; Kluwer: Dordrecht, The Netherlands, 2001. (b) *Aqueous-Phase Organometallic Catalysis*, 2nd ed.; Cornils, B., Herrmann, W. A., Eds.; Wiley-VCH: Weinheim, Germany, 1998. (c) Joó, F.; Kathó, Á. In *Handbook of Green Chemistry: Reactions in Water*; Li, C.-J., Ed.; Wiley-VCH: Weinheim, Germany, 2010; pp 389–408. (d) *Metal-Catalyzed Reactions in Water*; Dixneuf, P. H., Cadierno, V., Eds.; Wiley-VCH: Weinheim, Germany, 2013. (e) *Multiphase Homogeneous Catalysis*; Cornils, B., Herrmann, W. A., Horváth, I. T., Leitner, W., Mecking, S., Olivier-Bourbigou, H., Vogt, D., Eds.; Wiley-VCH: Weinheim, Germany, 2005. (f) Joó, F. Biphasic Catalysis-Homogeneous. In *Encyclopedia of Catalysis*, 2nd ed.; Horváth, I. T., Ed.; Wiley: New York, 2010 (published online); DOI: 10.1002/0471227617.

(13) (a) *Applied Homogeneous Catalysis with Organometallic Compounds*, Cornils, B., Herrmann, W. A., Eds.; Wiley-VCH: Weinheim, Germany, 1996. (b) Beller, M.; Cornils, B.; Frohning, C. D.; Kohlpaintner, C. W. *J. Mol. Catal. A: Chem.* **1995**, *104*, 17–85. (c) *Rhodium Catalyzed Hydroformylation*; van Leeuwen, P. W. N. M., Claver, C., Eds.; Kluwer: Dordrecht, The Netherlands, 2000; Catalysis by Metal Complexes Vol. 22. (d) Cornils, B. *Top. Curr. Chem.* **1999**,

- 206, 133–152. (e) Trzeciak, A. M.; Ziółkowski, J. J. *Coord. Chem. Rev.* **1999**, *190–192*, 883–900. (f) Lu, S. M.; Alper, H. J. *Am. Chem. Soc.* **2003**, *125*, 13126–13131. (g) Breit, B. In *Metal Catalyzed Reductive C–C Bond Formation*; Krische, M. J., Ed.; Springer: Berlin, Heidelberg, Germany, 2007; Vol. 279, pp 139–172. (h) Joó, F.; Kathó, Á. *J. Mol. Catal. A* **1997**, *116*, 3–26.
- (14) (a) Joó, F.; Kathó, Á. In *Handbook of Homogeneous Hydrogenation*; de Vries, J. G., Elsevier, C. J., Eds.; Wiley-VCH: Weinheim, Germany, 2007; Vol. 3, Chapter 38, pp 1327–1359. (b) Joó, F. In *Science of Synthesis: Water in Organic Synthesis*; Kobayashi, S., Ed.; Georg Thieme Verlag: New York, 2012; pp 95–119. (c) Kovács, G.; Ujaque, G.; Lledós, A.; Joó, F. *Eur. J. Inorg. Chem.* **2007**, *12*, 2879–2889. (d) Delhomme, C.; Schaper, L.-A.; Zhang-Presse, M.; Raudaschl-Sieber, G.; Weuster-Botz, D.; Kuehn, F. E. *J. Organomet. Chem.* **2013**, *724*, 297–299. (e) Papp, G.; Horváth, H.; Laurenczy, G.; Szatmári, I.; Kathó, Á.; Joó, F. *Dalton Trans.* **2013**, *42*, 521–529. (f) Chaloner, P. A.; Esteruelas, M. A.; Joó, F.; Oro, L. A. *Homogeneous Hydrogenation*; Kluwer: Dordrecht, The Netherlands, 1994.
- (15) (a) García-Álvarez, J.; García-Garrido, S. E.; Crochet, P.; Cadierno, V. *Curr. Top. Catal.* **2012**, *10*, 35–56. (b) Uma, R.; Crévisy, C.; Grée, R. *Chem. Rev.* **2003**, *103*, 27–51. (c) Cadierno, V.; Crochet, P.; Gimeno, J. *Synlett* **2008**, *8*, 1105–1124. (d) Crochet, P.; Díez, J.; Fernández-Zúmel, M. A.; Gimeno, J. *Adv. Synth. Catal.* **2006**, *348*, 93–100. (e) Campos-Malpartida, T.; Fekete, M.; Kathó, Á.; Joó, F.; Romerosa, A.; Saoud, M.; Wojtków, W. *J. Organomet. Chem.* **2008**, *693*, 468–474. (f) Csabai, P.; Joó, F. *Organometallics* **2004**, *23*, 5640–5643.
- (16) (a) Beletskaya, I. P.; Cheprakov, A. V. *Chem. Rev.* **2000**, *100*, 3009–3066. (b) Shaughnessy, K. H.; DeVasher, R. B. *Curr. Org. Chem.* **2005**, *9*, 585–604. (c) Bakherad, M. *Appl. Organomet. Chem.* **2012**, *27*, 125–140. (d) Wu, L.; Zhang, X.; Tao, Z. *Catal. Sci. Technol.* **2012**, *2*, 707–710. (e) Kumbhar, A.; Jadhav, S.; Kamble, S.; Rashinkar, G.; Salunkhe, R. *Tetrahedron Lett.* **2013**, *54*, 1331–1337. (f) *Applied Cross-Coupling Reactions*; Nishihara, Y., Ed.; Springer: Berlin, Heidelberg, 2013. (g) Shaughnessy, K. H. *Metal-Catalyzed Cross-Couplings of Aryl Halides to Form C–C Bonds in Aqueous Media*. In *Metal-Catalyzed Reactions in Water*; Dixneuf, P. H., Cadierno, V., Eds.; Wiley-VCH: Weinheim, Germany, 2013; pp 1–46.
- (17) (a) Berry, K. J.; Moya, F.; Murray, K. S.; van den Bergen, A. M. B.; West, B. O. *J. Chem. Soc., Dalton Trans.* **1982**, 109–116. (b) Haikarainen, A.; Sipilä, J.; Pietikäinen, P.; Pajunen, A.; Mutikainen, I. *Dalton Trans.* **2001**, *7*, 991–995. (c) Bahramian, B.; Mirkhani, V.; Tangestaninejad, S.; Moghadam, M. *J. Mol. Catal. A: Chem.* **2006**, *1–2*, 139–145. (d) Salanti, A.; Orlandi, M.; Tolppa, E.; Zoia, L. *Int. J. Mol. Sci.* **2010**, *11*, 912–926. (e) Allard, M.; Ricoux, R.; Guillot, R.; Mahy, J.-P. *Inorg. Chim. Acta* **2012**, *382*, 59–64. (f) Wang, X.; Wu, G.; Wang, F.; Ding, K.; Zhang, F.; Liu, X.; Xue, Y. *Catal. Commun.* **2012**, *28*, 73–76.
- (18) Wu, Z.; Zhou, L.; Jiang, Z.; Wu, D.; Li, Z.; Zhou, X. *Eur. J. Org. Chem.* **2010**, *26*, 4971–4975.
- (19) Yu, L.; Zhou, X.; Wu, D.; Xiang, H. *J. Organomet. Chem.* **2012**, *705*, 75–78.
- (20) Vanalabhpatana, P.; Peters, D. J. *Tetrahedron Lett.* **2003**, *44*, 3245–3247.
- (21) (a) Correia, I.; Costa Pessoa, J.; Veiros, L. F.; Jackusch, T.; Dornyei, A.; Kiss, T.; Castro, M. M. C. A.; Gerald, C. F. G. C.; Aveilla, F. *Eur. J. Inorg. Chem.* **2005**, *4*, 732–744. (b) Delahaye, É.; Diop, M.; Welter, R.; Boero, M.; Massobrio, C.; Rabu, P.; Rogez, G. *Eur. J. Inorg. Chem.* **2010**, *28*, 4450–4461.
- (22) (a) Egami, H.; Katsuki, T. *J. Am. Chem. Soc.* **2009**, *131*, 6082–6083. (b) Matsumoto, K.; Oguma, T.; Katsuki, T. *Angew. Chem., Int. Ed.* **2009**, *48*, 7432–7435. (c) Xiong, D.; Wu, M.; Wang, S.; Li, F.; Xia, C.; Sun, W. *Tetrahedron: Asymmetry* **2010**, *21*, 374–378. (d) Egami, H.; Oguma, T.; Katsuki, T. *J. Am. Chem. Soc.* **2010**, *132*, 5886–5895. (e) Kunisu, T.; Oguma, T.; Katsuki, T. *J. Am. Chem. Soc.* **2011**, *133*, 12937–12939. (f) Bryliakov, K. P.; Talsi, E. P. *Eur. J. Org. Chem.* **2011**, 4693–4698. (g) Matsumoto, K.; Egami, H.; Oguma, T.; Katsuki, T. *Chem. Commun.* **2012**, *48*, 5823–5825.
- (23) (a) Cohen, A.; Kopilov, J.; Lamberti, M.; Venditto, V.; Kol, M. *Macromolecules* **2010**, *43*, 1689–1691. (b) Ding, L.; Chu, Z.; Chen, L.; Lü, X.; Yan, B.; Song, J.; Fan, D.; Bao, F. *Inorg. Chem. Commun.* **2011**, *14*, 573–577. (c) Darensbourg, D. J.; Poland, R. R.; Strickland, A. L. *J. Polym. Sci., Polym. Chem.* **2012**, *50*, 127–133. (d) Cross, E. D.; Allan, L. E. N.; Decken, A.; Shaver, M. P. *J. Polym. Sci., Polym. Chem.* **2013**, *51*, 1137–1146. (e) Liu, J.; Bao, Y. Y.; Liu, Y.; Ren, W. M.; Lu, X. B. *Polym. Chem.* **2013**, *4*, 1439–1444.
- (24) (a) van der Drift, R. C.; Bouwman, E.; Drent, E. *J. Organomet. Chem.* **2002**, *650*, 1–24. (b) Martín-Matute, B.; Bogár, K.; Edin, M.; Kaynak, F. B.; Bäckvall, J. E. *Chem. Eur. J.* **2005**, *11*, 5832–5842. (c) Lorenzo-Luis, P.; Romerosa, A.; Serrano-Ruiz, M. *ACS Catal.* **2012**, *2*, 1079–1086. (d) Ahlsten, N.; Bartoszewicz, A.; Martín-Matute, B. *Dalton Trans.* **2012**, *41*, 1660–1670.
- (25) (a) Cadierno, V.; Francos, J.; Gimeno, J.; Nebra, N. *Chem. Commun.* **2007**, 2536–2538. (b) Kim, J. W.; Koike, T.; Kotani, M.; Yamaguchi, K.; Mizuno, N. *Chem. Eur. J.* **2008**, *14*, 4104–4109. (c) Cadierno, V.; Crochet, P.; Francos, J.; García-Garrido, S. E.; Gimeno, J.; Nebra, N. *Green Chem.* **2009**, *11*, 1992–2000. (d) Mantilli, L.; Mazet, C. *Tetrahedron Lett.* **2009**, *50*, 4141–4144. (e) Díaz-Álvarez, A. E.; Crochet, P.; Cadierno, V. *Catal. Commun.* **2011**, *13*, 91–96. (f) Wu, R.; Beauchamps, M. G.; Laquidara, J. M.; Sowa, J. R., Jr. *Angew. Chem., Int. Ed.* **2012**, *51*, 2106–2110.
- (26) (a) Fekete, M.; Joó, F. *Catal. Commun.* **2006**, *7*, 783–786. (b) González, B.; Lorenzo-Luis, P.; Serrano-Ruiz, M.; Papp, É.; Fekete, M.; Csépe, K.; Ósz, K.; Kathó, Á.; Joó, F.; Romerosa, A. *J. Mol. Catal. A: Chem.* **2010**, *326*, 15–20. (c) Udvardy, A.; Bényei, A. Cs.; Kathó, Á. *J. Organomet. Chem.* **2012**, *717*, 116–122. (d) Menéndez-Rodríguez, L.; Crochet, P.; Cadierno, V. *J. Mol. Catal. A: Chem.* **2013**, *366*, 390–399.
- (27) (a) Botsivali, M.; Evans, D. F.; Missen, P. H.; Upton, M. W. *J. Chem. Soc., Dalton Trans.* **1985**, 1147–1149. (b) Evans, D. F.; Missen, P. H. *J. Chem. Soc., Dalton Trans.* **1987**, 1279–1281.
- (28) (a) Borer, L.; Thalken, L.; Ceccarelli, C.; Glick, M.; Zhang, J. H.; Reiff, W. M. *Inorg. Chem.* **1983**, *22*, 1719–1724. (b) Xia, H.-T.; Liu, Y.-F.; Yang, S.-P.; Wang, D.-Q. *Acta Crystallogr., Sect. E* **2006**, *62*, 5864–5865. (c) Higham, C. S.; Dowling, D. P.; Shaw, J. L.; Cetin, A.; Ziegler, C. J.; Farrell, J. R. *Tetrahedron Lett.* **2006**, *47*, 4433–4436. (d) Xie, Y.; Liu, Q.; Jiang, H.; Ni, J. *Eur. J. Inorg. Chem.* **2003**, *22*, 4010–4016.
- (29) Xu, Y.-M.; Gao, S.; Weng, Ng, S. *Acta Crystallogr., Sect. E* **2009**, *65*, 3150–3151.
- (30) (a) Joó, F.; Kovács, J.; Bényei, A. Cs.; Kathó, Á. *Catal. Today* **1998**, *42*, 441–448. (b) Joó, F.; Kovács, J.; Bényei, A. Cs.; Kathó, Á. *Angew. Chem., Int. Ed. Engl.* **1998**, *37*, 969–970. (c) Grosselin, J. M.; Mercier, C.; Allmang, G.; Grass, F. *Organometallics* **1991**, *10*, 2126–2133.
- (31) (a) Schumann, H.; Ravindar, V.; Larisa, M.; Baidossi, W.; Sasson, Y.; Blum, J. *J. Mol. Catal. A: Chem.* **1997**, *118*, 55–61. (b) Schulz, J.; Cisařová, I.; Štěpnička, P. *Eur. J. Inorg. Chem.* **2012**, 5000–5010. (c) Sahoo, S.; Lundberg, H.; Edén, M.; Ahlsten, N.; Wan, W.; Zou, X.; Martín-Matute, B. *ChemCatChem* **2012**, *4*, 243–250.
- (32) (a) García-Álvarez, J.; Gimeno, J.; Suárez, F. J. *Organometallics* **2011**, *30*, 2893–2896. (b) Díez, J.; Gimeno, J.; Lledós, A.; Suárez, F. J.; Vicent, C. *ACS Catal.* **2012**, *2*, 2087–2099.
- (33) (a) Cadierno, V.; García-Garrido, S. E.; Gimeno, J.; Varela-Álvarez, A.; Sordo, J. A. *J. Am. Chem. Soc.* **2006**, *128*, 1360–1370. (b) Liu, P. N.; Kun, D. J.; Lau, C. P. *Adv. Synth. Catal.* **2011**, *353*, 275–280.
- (34) (a) Kraus, M. *Collect. Czech. Chem. Commun.* **1972**, *37*, 460–465. (b) Freidlin, L. K.; Kopyttsev, Y. A.; Nazarova, N. M. *Russ. Chem. Bull.* **1972**, *11*, 1347–1354. (c) Lu, X.; Ji, J.; Ma, D.; Shen, W. *J. Org. Chem.* **1991**, *56*, 5774–5778. (d) Sadeghmoghaddam, E.; Gu, H.; Shon, Y.-S. *ACS Catal.* **2012**, *2*, 1838–1845. (e) Sadeghmoghaddam, E.; Galeb, K.; Shon, Y.-S. *Appl. Catal. A: Gen.* **2011**, *405*, 137–141. (f) Moreno, M.; Kissell, L. N.; Jasinski, J. B.; Zamborini, F. P. *ACS Catal.* **2012**, *2*, 2602–2613.
- (35) Sasson, Y.; Zoran, A.; Blum, J. *J. Mol. Catal.* **1981**, *11*, 293–300.
- (36) de Bellefon, C.; Caravieilh, S.; Kuntz, E. G. C. R. *Acad. Sci. Paris, Ser. IIC, Chim.* **2000**, *3*, 607–614.

(37) (a) Conradie, J.; Ghosh, A. *J. Phys. Chem. B* **2007**, *111*, 12621–12624. (b) Scheurer, A.; Puchta, R.; Hampel, F. *J. Coord. Chem.* **2010**, *63*, 2868–2878. (c) Sheikhshoaie, M.; Shamspur, T.; Mohammadi, S. *Z. J. Chem. Pharm. Res.* **2012**, *4*, 27–32. (d) Zhou, H.-B.; Wang, H.-S.; Chen, Y.; Xu, Y.-L.; Song, X.-J.; Song, Y.; Zhang, Y.-Q.; You, X.-Z. *Dalton Trans.* **2011**, *40*, 5999–6006.

(38) Adão, P.; Pessoa, J. C.; Henriques, R. T.; Kuznetsov, M. L.; Aveçilla, F.; Maurya, M. R.; Kumar, U.; Correia, I. *Inorg. Chem.* **2009**, *48*, 3542–3561.

(39) (a) van Belzen, R.; Elsevier, J. C.; Dedieu, A.; Veldman, N.; Spek, A. L. *Organometallics* **2003**, *22*, 722–736. (b) Alonso, E.; Casas, J. M.; Fornies, J.; Fortuño, C.; Martín, A.; Orpen, A. G.; Tsipis, C. A.; Tsipis, A. C. *Organometallics* **2001**, *20*, 5571–5582.

(40) Comas-Vives, A.; González-Arellano, C.; Boronat, M.; Corma, A.; Iglesias, M.; Sánchez, F.; Ujaque, G. *J. Catal.* **2008**, *254*, 226–237.

(41) (a) Smith, K.-J.; Norton, J. R.; Tilset, M. *Organometallics* **1996**, *15*, 4515–4520. (b) Václavík, J.; Kuzma, M.; Prech, J.; Kacer, P. *Organometallics* **2011**, *30*, 4822–4829.

(42) Joubert, J.; Delbecq, F. *Organometallics* **2006**, *4*, 854–861.

(43) Bellarosa, L.; Díez, J.; Gimeno, J.; Lledós, A.; Suárez, F. J.; Ujaque, G.; Vicent, C. *Chem. Eur. J.* **2012**, *18*, 7749–7765.

(44) Altomare, A.; Cascarano, G.; Giacobuzzo, C.; Guagliardi, A. *J. Appl. Crystallogr.* **1993**, *26*, 343–350.

(45) Sheldrick, G. M. *Acta Crystallogr., Sect. A* **2008**, *A64*, 112–122.

(46) Farrugia, L. J. *J. Appl. Crystallogr.* **1999**, *32*, 837–838.

(47) Hiehl, H.; Hach, C. C. *Inorg. Synth.* **1950**, *3*, 196–201.

(48) Frisch, M. J.; Trucks, G. W.; Schlegel, H. B.; Scuseria, G. E.; Robb, M. A.; Cheeseman, J. R.; Scalmani, G.; Barone, V.; Mennucci, B.; Petersson, G. A.; Nakatsuji, H.; Caricato, M.; Li, X.; Hratchian, H. P.; Izmaylov, A. F.; Bloino, J.; Zheng, G.; Sonnenberg, J. L.; Hada, M.; Ehara, M.; Toyota, K.; Fukuda, R.; Hasegawa, J.; Ishida, M.; Nakajima, T.; Honda, Y.; Kitao, O.; Nakai, H.; Vreven, T.; Montgomery, J. A., Jr.; Peralta, J. E.; Ogliaro, F.; Bearpark, M.; Heyd, J. J.; Brothers, E.; Kudin, K. N.; Staroverov, V. N.; Kobayashi, R.; Normand, J.; Raghavachari, K.; Rendell, A.; Burant, J. C.; Iyengar, S. S.; Tomasi, J.; Cossi, M.; Rega, N.; Millam, N. J.; Klene, M.; Knox, J. E.; Cross, J. B.; Bakken, V.; Adamo, C.; Jaramillo, J.; Gomperts, R.; Stratmann, R. E.; Yazyev, O.; Austin, A. J.; Cammi, R.; Pomelli, C.; Ochterski, J. W.; Martin, R. L.; Morokuma, K.; Zakrzewski, V. G.; Voth, G. A.; Salvador, P.; Dannenberg, J. J.; Dapprich, S.; Daniels, A. D.; Farkas, Ö.; Foresman, J. B.; Ortiz, J. V.; Cioslowski, J.; Fox, D. J. *Gaussian 09, Revision A.1*; Gaussian, Inc., Wallingford, CT, 2009.

(49) (a) Tomasi, J.; Mennucci, B.; Cammi, R. *Chem. Rev.* **2005**, *105*, 2999–3093. (b) Scalmani, G.; Frisch, M. J. *J. Chem. Phys.* **2010**, *111*, 114110–114125.

(50) (a) Becke, A. D. *J. Chem. Phys.* **1993**, *98*, 5648–5652. (b) Lee, C.; Yang, W.; Parr, R. G. *Phys. Rev. B* **1988**, *37*, 785–789.

(51) Zhao, Y.; Truhlar, D. G. *Theor. Chem. Acc.* **2008**, *120*, 215–241.

(52) Grimme, S. *J. Chem. Phys.* **2006**, *3*, 034108–034116.

(53) (a) Krishnan, R.; Binkley, J. S.; Seeger, R.; Pople, J. A. *J. Chem. Phys.* **1980**, *8*, 4654–4656. (b) McLean, A. D.; Chandler, G. S. *J. Chem. Phys.* **1980**, *10*, 5639–5648. (c) Hehre, W. J.; Ditchfield, R.; Pople, J. A. *J. Chem. Phys.* **1972**, *5*, 2257–2261. (d) Hariharan, P. C.; Pople, J. A. *Theor. Chim. Acta* **1973**, *28*, 213–222. (e) Francl, M. M.; Pietro, W. J.; Hehre, W. J.; Binkley, J. S.; DeFrees, D. J.; Pople, J. A.; Gordon, M. S. *J. Chem. Phys.* **1982**, *7*, 3654–3665.

(54) (a) Hay, P. J.; Wadt, W. R. *J. Chem. Phys.* **1985**, *1*, 270–283. (b) Wadt, W. R.; Hay, P. J. *J. Chem. Phys.* **1985**, *82*, 284–298.

(55) Andrae, D.; Häußermann, U.; Dolg, M.; Stoll, H.; Preuß, H. *Theor. Chim. Acta* **1990**, *77*, 123–141.

(56) Hurlley, M. M.; Pacios, L. F.; Christiansen, P. A.; Ross, R. B.; Emler, W. C. *J. Chem. Phys.* **1986**, *12*, 6840–6853.

(57) (a) Peng, C.; Ayala, P. Y.; Schlegel, H. B.; Frisch, M. J. *J. Comput. Chem.* **1996**, *17*, 49–56. (b) Peng, C.; Schlegel, H. B. *Isr. J. Chem.* **1994**, *33*, 449–454.